

# Structure of polydisperse inverse ferrofluids: Theory and computer simulation

Y. C. Jian and J. P. Huang\*

*Surface Physics Laboratory (National key laboratory) and Department of Physics,  
Fudan University, Shanghai 200433, China*

R. Tao

*Department of Physics, Temple University,  
Philadelphia, Pennsylvania 19122, USA*

## Abstract

By using theoretical analysis and molecular dynamics simulations, we investigate the structure of colloidal crystals formed by nonmagnetic particles (or *magnetic holes*) suspended in ferrofluids (also called *inverse ferrofluids*), by taking into account the effect of polydispersity in size of the particles. Such polydispersity often exists in real situations. We obtain an analytical expression for the interaction energy of monodisperse, bidisperse, and polydisperse inverse ferrofluids. BCT (body-centered tetragonal) lattices are shown to possess the lowest energy when compared with other sorts of lattices, and thus serve as the ground state of the systems. Also, the effect of particle size distributions (namely, polydispersity in size) plays an important role in the formation of various kinds of structural configurations. Thus, it seems possible to fabricate colloidal crystals by choosing appropriate polydispersity in size.

PACS numbers: 61.20.Gy, 75.50.Mm, 82.70.Dd

---

\* Electronic address: jphuang@fudan.edu.cn

## I. INTRODUCTION

In recent years, inverse ferrofluids with nonmagnetic colloidal particles suspended in a ferrofluid have drawn considerable attention for its potential application in its industrial applications and potential use in biomedicine [1, 2, 3, 4, 5, 6, 7, 8]. The size of the nonmagnetic particles are about  $1 \sim 100 \mu\text{m}$ , which can be easily made in experiments, such as polystyrene particles. The inverse ferrofluid system can be modelled in the dipolar approximation. The induced dipolar interaction could be used to explain the crystallization of nonmagnetic particles and nonlinear magnetic phenomena [9, 10] in the presence of constant or oscillating magnetic fields. This interaction potential through the external magnetic field between the particles induces the chain formation and transition from liquid to solid-like behavior, and makes it possess the phase transition and aggregation behavior similar to electrorheological and magnetorheological fluids [11, 12]. Tao and Sun first theoretically suggested the ground state of microcrystalline structures in electrorheological and magnetorheological fluids to be a body-centered tetragonal (bct) lattice by using the dipolar interaction approximation [13]. The possible ground configuration is the one which minimizes the dipole interaction energy. It was then confirmed by the simulations and experiments [14, 15, 16, 17, 18]. The followed multipole-expansion theory [19] gives an accurate analytical expression for many-particle cases [20], as a useful improvement of the dipolar approximation. Sun and Yu considered polydisperse electrorheological fluids in which the particles have dielectric contrasts [14, 21]. Also, the effect of size distribution on configurations under a static yield stress or viscoelastic force was calculated for electrorheological and magnetorheological fluids [22, 23].

In this work, we shall use the dipole-multipole force model [24] to investigate the structure of inverse ferrofluids. The leading dipole-dipole force does not reflect the geometry relation between the particles nearby, while the dipole-multipole model includes the contributions from the size mismatch and is simpler and practical than the multipolar expansion theory [19, 20] in dealing with the complex interaction between particles for its accuracy. Size distributions can be regarded as a crucial factor which causes depletion forces in colloidal droplets [25]. As a matter of fact, polydispersity in size of particles often exists in real situations, since the particles always possess a Gaussian or log-normal distribution. Here we consider size distributions as an extra factor affecting the interaction energy. Polydisperse ferrofluid models are usually treated in a global perspective using chemical potential or free energy methods [3, 26, 27], while the current model

concerns the local nature in the crystal background. A brief modeling is carried out for the size distribution picture in the formation of crystal lattices. The purpose of this paper is to use this model to treat the structure formation in monodisperse, bidisperse, and polydisperse inverse ferrofluids, thus yielding theoretical predictions for the ground state for the systems with or without particle size distributions (or polydisperseity in size). It is found that when the size mismatch is considered between the particles, the interaction between them becomes complex and sensitive to the different configurations. This method can also be extended to other ordered configurations in polydisperse crystal systems.

This paper is organized as follows. In Section II, based on the dipole-multipole force model [24], we present the basic two-particle interaction model to derive interaction potentials. In Sections III and IV, we apply the model to three typical structures of colloid crystals formed in inverse ferrofluids, and then investigate the ground state in two different configurations by taking into account the effect of size distributions. As an illustration, in Section V we perform molecular dynamics simulations to give a picture of the particle size distribution in the formation of a bct lattice in bidisperse inverse ferrofluids. The paper ends with a discussion and conclusion in Section VI.

## II. INTERACTION MODEL FOR TWO NONMAGNETIC PARTICLES

We start by considering a simple situation in which two nonmagnetic spherical particles (or called *magnetic holes*) are put nearby inside a ferrofluid which is homogeneous at the scale of a sphere in an applied uniform magnetic field  $H$ , see Fig. 1. The nonmagnetic particles create holes in the ferrofluid, and corresponding to the amount and susceptibility of the ferrofluid, they possess the magnetic moment. When the two particles placed together with distance  $r_{ij}$  away, we can view the magnetization in one sphere(labeled as A) is induced by the second(B). The central point of dipole-multipole technique is to treat B as the dipole moment  $m$  at the first place, and then examine the the surface charge density  $\sigma$  induced on the sphere A. From  $\sigma$  we can use the multipole expansion (detailed discussion in [28]) to obtain the multipole moment  $A_{ln}$ . When exchanging the status of A and B, treating A as the dipole moment, the averaged force between the two particles is thus obtained. For the perturbation of the magnetic field due to the two particles, magnetization  $M$  in the particles become nonuniform, and they will obtain multipole moments from mutual induction. However, the bulk magnetic charge density still satisfies  $\rho = \nabla \cdot M = 0$ , and the

magnetic moment can be well described by  $m = V \frac{3MH}{2M+3H} = V \frac{\chi_f}{1+\frac{2}{3}\chi_f} H = V\chi H$ , where  $\chi_f$  (or  $\chi$ ) means the magnetic susceptibility of the host (or inverse) ferrofluid. So we need only study the surface charge  $\sigma_n$ , expanding it in Legendre polynomials in the spherical coordinates  $(r, \phi, \varphi)$  [24]:

$$\sigma_n(\cos \phi) = \frac{\chi}{r_{ij}^3} \sum_{l=1}^{\infty} l(l+1) \left(\frac{r_1}{r_{ij}}\right)^{l-1} P_l(\cos \phi), \quad (1)$$

where  $r_1$  denotes the radius of the particle and the dipole moment is induced in a distance  $r_{ij}$  away. The  $l \geq 2$  part in Eq. (1) contributes to higher multipole effect. Thus the multipole moments in spherical coordinates can be written as  $A_{ln} = \int Y_{ln}^*(\phi, \varphi) r_1^l \sigma_n dS$ . [25, 28] Here we set spherical harmonics  $\int_0^{2\pi} d\varphi \int_0^\pi \sin \phi Y_{l',n'}^*(\phi, \varphi) Y_{l,n}(\phi, \varphi) = \delta_{l',l} \delta_{n',n}$ . If we consider the rotational symmetry around the direction of magnetization  $M$ , the force between the dipole moment  $m$  and induced multipole moment  $A_{ln}$  can be derived as

$$F_{D-M} = (-1)^l (l+1)(l+2) \left(\frac{4\pi}{2l+1}\right)^{\frac{1}{2}} \frac{mA_{ln}}{r_{ij}^{l+3}} \cos \phi. \quad (2)$$

In view of the orthogonal relation  $\int_{-1}^1 P_l^n P_{l'}^n dx = \frac{2}{2l+1} \frac{(l+n)!}{(l-n)!} \delta_{ll'}$ , we obtain the interaction energy for the dipole-multipole moment

$$U_{D-M} = \frac{\pi}{4} \mu_f m_1 m_2 \sum_l \frac{\pi}{2} \chi \frac{l(l+1)^2}{2l+1} (r_1^{2l+1} + r_2^{2l+1}) \frac{1 - 3 \cos^2 \theta}{r_{ij}^{2l+4}} = \mu \sum_l f(l) \frac{1 - 3 \cos^2 \theta}{r_{ij}^{2l+4}}, \quad (3)$$

where  $\mu = \frac{\pi}{4} \mu_f m_1 m_2$ ,  $f(l) = \frac{\pi}{2} \chi \frac{l(l+1)^2}{2l+1} (r_1^{2l+1} + r_2^{2l+1})$ , the suffix  $D$  ( $M$ ) of force  $F$  or energy  $U$  stands for the dipole moment (multipole moment), and magnetic permeability  $\mu_f = \mu_0(1 + \chi_f)$  with  $\mu_0 = 4\pi \times 10^{-7} \text{ H}\cdot\text{m}^{-1}$ . Here  $m_1$  and  $m_2$  denote the magnetic moments of the two particles, which is induced by external field as dipolar perturbation.  $0 \leq \theta \leq \frac{\pi}{2}$  is the angle between the their joint line with the direction of external field, and  $\phi$  and  $\varphi$  are both the spherical coordinates  $(r, \phi, \varphi)$  for one single particle. For typical ferrofluids, there are magnetic susceptibilities,  $\chi_f = 1.9$  and  $\chi = 0.836$  [27]. Because we consider the bct, fcc, hcp lattices, the crystal rotational symmetry in the xy plane is fourfold, and the value of  $n$  can only be  $0, \pm 4, \dots$  [6]. In the general case, when the polarizabilities between the particles and ambient fluid is low, the higher magnetic moments can be neglected since they contribute less than 5 percent of the total energy [24]. In this picture, the particle pair reflects the dipole-dipole and dipole-multipole nature of the interaction, and can be used to predict the behavior of particle chains in simple crystals.

### III. POSSIBLE GROUND STATE FOR UNIFORM ORDERED CONFIGURATIONS

Let us first consider a bidisperse model which has been widely used in the study of magnetorheological fluids and ferrofluids. The model has large amount of spherical nonmagnetic particles with two different sizes suspended in a ferrofluid which is confined between two infinite parallel nonmagnetic plates with positions at  $z = 0$  and  $z = L$ , respectively. When a magnetic field is applied, dipole and multipole moments will be induced to appear in the spheres. The inverse ferrofluid systems consist of spherical nonmagnetic particles in a carrier ferrofluid, whose viscosity increases dramatically in the presence of an applied magnetic field. If the magnetic field exceeds a critical value, the system turns into a solid whose yield stress increases as the exerting field is further strengthened. The induced solid structure is supposed to be the configuration minimizing the interaction energy, and here we assumes first that the particles with two different size have a fixed distribution as discussed below.

Using the cylindric coordinates, the interaction energy between two particles labelled as  $i$  and  $j$  considering both the dipole-dipole and dipole-multipole effects can be written as

$$U_{ij}(\rho, z) = \mu \left( 1 + \sum_l \frac{f(l)}{r_{ij}^{2l+1}} \right) \cdot \left( \frac{1 - 3 \cos^2 \theta}{r_{ij}^3} \right), \quad (4)$$

where the center-to-center separation  $r_{ij} = |r_i - r_j| = [\rho^2 + (z_i - z_j)^2]^{\frac{1}{2}}$ , and  $\theta$  is the angle between the field and separation vector  $r_{ij}$  (see Fig. 1). Here  $\rho = [(x_i - x_j)^2 + (y_i - y_j)^2]^{\frac{1}{2}}$  stands for the distance between chain  $A$  and chain  $B$  (Fig. 2), and  $z_i$  denotes the vertical shift of the position of particles. Since the inverse ferrofluid is confined between two plates, the particle dipole at  $(x, y, z)$  and its images at  $(x, y, 2Lj \pm z)$  for  $j = \pm 1, \pm 2, \dots$  constitute an infinite chain. In this work, we would discuss the physical infinite chains. After applying a strong magnetic field, the mismatch between the spheres and the host ferrofluid, as well as the different sizes of two sorts of spheres will make the spheres aggregate into a body-centered tetragonal (bct) lattice. We study the case in which the identical particles gather together to form a uniform chain, when phase separation or transition happens. In general, for a colloidal crystal, the individual colloidal particles are touching. However, if the colloidal particles are charged and stabilized by electric or magnetic static force, they can be made as nontouching. The interaction energy between the particles can be divided into two parts: one is from the self energy of one chain( $U_s$ ), the other is from the interation between different chains( $U_{ij}(\rho, z)$ ). Consider the particles along one chain at  $r_j = 2aj\hat{z}$  ( $j = 0, \pm 1, \pm 2, \dots$ ) (namely, chain A), and the other chain at  $r_j = (2j+1)a\hat{z}$  (chain B),

the average self energy per particle in an infinite chain is  $U_s = -\mu \sum_{s=1}^{\infty} \left[ \frac{1}{(2as)^3} + 2 \sum_l \frac{f(l)}{(2as)^{2l+4}} \right]$ .

If we notice that for an infinite chain all even multipole contributions vanish due to spatial magnetic antisymmetry around the spheres, the sum starts at  $l = 3$ . Because the radius of the sphere is smaller than the lattice parameter  $a$ , for large multipole moment,  $\frac{r_1^{2l+1} + r_2^{2l+1}}{(2a)^{2l}} \ll 1$ , we need only consider the first two moment contributions for simplicity. Thus the average self energy  $U_s$  can be calculated as  $U_s = -2\mu \left( \frac{\zeta(3)}{(2a)^3} + \frac{f(3)\zeta(6)}{(2a)^6} + \frac{f(5)\zeta(10)}{(2a)^{10}} \right) = -\mu \left( \frac{0.300514}{a^3} + \frac{0.0317920f(3)}{a^6} + \frac{0.00195507f(5)}{a^{10}} \right)$ , where  $\zeta(n) = \sum_{s=1}^{\infty} \frac{1}{s^n}$  is the Riemann  $\zeta$  function. The interaction energy between two parallel infinite chains can be given by  $\frac{1}{2}U_{ij}(\rho, z)$ , in which the particles along one chain locate at  $r_j = 2aj\hat{z}$  ( $j = 0, \pm 1, \pm 2, \dots$ ) and one particle locates at  $r_j = \rho + z\hat{z}$ ,

$$\begin{aligned} U_{ij}(\rho, z) &= -\mu \left[ (2 + \rho \frac{\partial}{\partial \rho}) \sum_{j=-\infty}^{\infty} \frac{1}{[\rho^2 + (z - 2ja)^2]^{\frac{3}{2}}} \right. \\ &\quad \left. - \mu \left[ \sum_l f(l) \left( 2 + \frac{3}{2l+2} \rho \frac{\partial}{\partial \rho} \right) \sum_{j=-\infty}^{\infty} \frac{1}{[\rho^2 + (z - 2ja)^2]^{l+2}} \right] \right] \\ &= U_1 + U_2. \end{aligned} \quad (5)$$

Following the Fourier expanding technique which is proposed by Tao *et al.* [13], we derive  $U_2$  which is the second part of  $U_{ij}(\rho, z)$  as

$$U_2 = -\mu \sum_l \frac{f(l)}{4a\rho^{2l+3}} \left[ -\frac{(2l+1)\sqrt{\pi}\Gamma(l+\frac{3}{2})}{\Gamma(l+3)} + 2^{\frac{1}{2}-l} \left( \frac{s\rho}{a} \right)^{l+\frac{3}{2}} \pi^{l+2} \cos\left(\frac{s\pi z}{a}\right) \cdot S \right] \quad (6)$$

with

$$S = \sum_{s=1}^{\infty} \left( \frac{K_{\frac{5}{2}}\left(\frac{s\pi}{\rho}\right)}{\Gamma(l+3)} + \frac{4K_{\frac{3}{2}}\left(\frac{s\pi}{\rho}\right)}{\Gamma(l+2)} \right). \quad (7)$$

Here  $K_i(x)$  represents the  $i$ th order modified bessel function,  $\Gamma(x)$  the  $\Gamma$  function, and  $s$  denotes the index in Fourier transformation [13]. Combining the dipole-dipole energy  $U_1$ , which is written as

$$U_1 = -\frac{\mu}{a^3} \sum_{s=1}^{\infty} 2\pi^2 s^2 K_0\left(\frac{s\pi\rho}{a}\right) \cos\left(\frac{s\pi z}{a}\right). \quad (8)$$

Thus, we obtain the expression for  $U_{ij}(\rho, z)$ , and the interaction energy per particle  $U(\rho, z)$  is  $U_s + \frac{1}{2} \sum_k U_{ij}(\rho, z)$ , where  $\sum_k$  denotes the summation over all chains except the considered particle. For the same reason of approximation discussed above, we need only choose the first two term ( $l = 3$  and  $l = 5$ ) in the calculation.

The interaction between chain A and chain B depends on the shift  $z$ , the lattice structure and the particle size. An estimation of the interaction energy per particle includes the nearest and

next-nearest neighboring chains, here we could discuss three most common lattice structures: bcc, fcc (face-centered cubic), and hcp (hexagonal close-packed) lattices. For the above lattices, their corresponding energy of  $U_{ij}(\rho, z)$  can be respectively approximated as  $U_{ij,bct}(\rho, z) = 4U_{ij}(\sqrt{3}a, z = 0) - 4U_{ij}(\sqrt{6}a, z = 0)$ ,  $U_{ij,fcc}(\rho, z) = 4U_{ij}(\sqrt{3}a, z = 0) - 2U_{ij}(2a, z = 0)$ , and  $U_{ij,hcp}(\rho, z) = 3U_{ij}(\sqrt{3}a, z = 0) - 4U_{ij}(2a, z = 0)$ .

Figure 3 shows, for different lattices, the dependence of  $U_{ij}(\rho, z)$  on the vertical position shift  $z$ , which determines whether the interaction is attractive or repulsive.  $U_{ij}(\rho, z)$  reflects the energy difference between chain A and chain B for (a) bct, (b) fcc, and (c) hcp lattices. It is evident that, for the same lattice structure,  $U_{ij}(\rho, z)$  is minimized when the size difference between chain A and chain B is the smallest. For the sake of comparison, we also plot the results obtained by considering the dipole-dipole interaction only. In the vicinity of the equilibrium point which pulls the particle to  $z = (2j + 1)a$ , the dipole-multipole effect enlarges the energy minimization and shows more stable intendance for the crystal system. Comparing the different lattices, we find that the bct lattice possesses the smallest energy at the equilibrium point, thus being the most stable.

Figure 4 displays the interaction energy  $U(\rho, z)$  as a function of the lattice constant  $a$  for the bct lattice. It is shown that as the lattice constant increases, the dipole-multipole effect becomes weaker and weaker, and eventually it reduces to the dipole-dipole effect. In other words, as the lattice constant is smaller, one should take into account the dipole-multipole effect. In this case, the effect of polydispersity in size can also play an important role.

Figure 5 displays the interaction energy per particle  $U(\rho, z)$  vs the lattice parameter  $a$  for different lattice structures. The bct structure also proves to be the most stable state while the hcp lattice has the highest energy. It also shows that the energy gap between bct lattice and fcc lattice exists but is small. Figure 6(a) shows that the energy gap  $\Delta U = U_{bct} - U_{fcc}$  is about 0.5 percent of the interaction energy value. In this aspect, the bct lattice proves always to be a more stable structure comparing with fcc. As the radius of particles increases, the energy gap between bct and fcc lattice enlarges accordingly. That is, the bct lattice becomes much more stable. Figure 6(b) shows the bct lattice energy  $U(\rho, z)$  in respect of different sizes of particles for chain A and chain B. It can be seen that the close touching packing ( $r_1 = r_2 = a$ ) has the lowest energy state. However, also from the graph, the crystal with the same particle size (monodisperse system) may not be the lowest energy state, which gives a possible way of fabricating different crystals by tuning the distribution of particle size.

#### IV. POLYDISPERSE SYSTEM WITH RANDOM DISTRIBUTIONS

In Section III, we have discussed the structure and interaction in a bidisperse inverse ferrofluid (namely, containing particles with two different sizes). But the interaction form in polydisperse crystal system is complex and sensitive to the microstructure in the process of crystal formation. Now we investigate the structure of polydisperse inverse ferrofluids with particles of different sizes in a random configuration. To proceed, we assume that the average radius  $r$  satisfies the Gaussian distribution

$$P(r) = \frac{1}{\sqrt{2\pi}\sigma} \exp\left(-\frac{(r - r_0)^2}{2\sigma^2}\right),$$

where  $\sigma$  denotes the standard deviation of the distribution of particle radius, which describes the degree of polydispersity. Integrating Eq. (6) by  $r_1$  and  $r_2$ , we could get the average dipole-multipole energy  $\bar{U}_2$ . Doing the same calculation to self energy  $U_s$ , we can get the average interaction energy  $\bar{U}(\rho, z) = \bar{U}_s + U_1 + \bar{U}_2$ , where the particle size  $r_1$  and  $r_2$  are replaced by the mean radius  $r_0$ . The particle sizes will be distributed in a wider range as long as a larger  $\sigma$  is chosen.

Figure 7(a) shows the ground state interaction energy of bct lattice for the above two configurations. As the degree of polydispersity  $\sigma$  increases, the energy  $U(\rho, z)$  drops fast, especially when the distribution of particle size gathers around  $r = a$ . It shows that the inverse ferrofluid crystal in the formation of ground state tends to include particles possessing more different sizes. The crystal configuration energy of two uniform chains with identical particle aggregating is also plotted in the graph. Here we consider two cases. First, we assume particles in chain A and chain B are identical,  $r_1 = r_2 = r_0$ . As  $r_0$  increases, the behavior of energy decreasing is discovered to be similar with the random configuration with  $\sigma = 0.2r_0$ . Second, we set for one chain, such as chain B, the particle size  $r_2 = a$  to be unchanged, while the particle size  $r_1$  of chain A increases. It shows that the bct lattice energy for the second case is lower than the first case and two other random configurations. And it also shows that the random configuration is not always the state with the lowest energy. It proves that polydisperse systems are sensitive to many factors which can determine the microstructure. In fact, in a more detailed calculation, the nonmagnetic particle will be elongated and the surface charge will have different distribution when a high magnetic field is applied. Figure 7(b) shows the energy gap between bct and fcc lattices for different distribution deviation  $\sigma$ . It is evident that higher  $\sigma$  leads to larger energy difference between bct and fcc, especially at larger  $r_0$ . In other words, at larger  $r_0$  and/or  $\sigma$ , bct lattices are much more stable than fcc.

## V. MOLECULAR-DYNAMIC SIMULATIONS

Here we use a molecular-dynamic simulation, which was proposed by Tao *et al.* [14], in order to briefly discuss the structure formation of bidisperse inverse ferrofluids. The simulation herein involves dipolar forces, multipole forces, vicious drag forces and the Brownian force. The particles are confined in a cell between two parallel magnetic pole plates, and they are randomly distributed initially, as shown in Fig. 8(a). The motion of a particle  $i$  is described using a Langevin equation,

$$m \frac{d^2 \vec{r}_i}{dt^2} = \vec{F}_i - 3\pi\sigma\eta \frac{d\vec{r}_i}{dt} + \vec{R}_i(t), \quad (9)$$

where  $3\pi\sigma\eta v_i$  is the Stokes's drag force,  $R_i$  is the Brownian force, and

$$F_i = \sum_{i \neq j} (f_{ij} + f_{ij}^{rep}) + f_i^{wall}. \quad (10)$$

Here  $f_{ij} = -\nabla U(\rho, z)$ , while  $f_{ij}^{rep}$ ,  $f_i^{wall}$ ,  $R_i(t)$ ,  $A'$ , and  $B'$  have the same expressions as those in Ref. [14] and the referees therein. Figure 8 shows the inverse ferrofluid structure with the parameters, temperature  $T = 0$  K,  $A' \equiv \frac{\mu_f m_1 m_2}{3\pi^2 \sigma^6 \eta^2} \cdot m = 10^{-2}$ , and  $B' \equiv \frac{\sqrt{6\pi k_B T \sigma^9 \eta / \tau}}{3\mu_f m_1 m_2} = 0$ , where  $m$  and  $\sigma$  are respectively the average mass and diameter of particles,  $k_B$  is Boltzmann constant and  $\tau$  is the subinterval time step. We choose small  $A'$  and  $B'$  to stimulate the ground state system under slight perturbation.

We take into account a bidisperses system that contains two kinds of particles with different sizes, as shown in Fig. 8. In details, this figure displays the configuration of particle distribution in a bidisperse system at (a) the initial state, (b) the state after 15000 time steps, and (c) the state after 80000 time steps. The orderness of Fig. 8(c) is better than Fig. 8(b). Here we should remark that, if the steps more than 80000 are calculated, the configuration keeps approximately the same as Fig. 8(c). The structure for the bi-disperse system in Fig. 8(b) and (c) has the following features: (i) In the field direction, the large spheres form the main chains from one plate to the other, where the large spheres touch each other. (ii) The large spheres also form many small bct lattice grains. However, they do not form a large bct lattice. (iii) The small spheres fill the gaps between these bct lattice grains. From Fig. 8, it is observed that, for the parameters currently used, the orderness of a bidisperse system (which is a bct-like structure) is not as good as that of monodisperse system (no configurations shown herein). Here we should also mention that the degree of orderness of a specific system depends on the physical parameters in use, as already displayed in Fig. 6. According to Fig. 6, we have found that the crystal with the same particle

size (monodisperse system) may not always be the lowest energy state, in view of various possible kinds of polydispersity. In fact, the formation of real crystals involves many complex factors which could affect the crystal lattice structure and the arrangement of particles with different physical or even chemical nature. For example, when the temperature is high, the Brownian force may have a dominated effect, thus changes the final state. Like the discussion in [16], when increasing the constant  $B'$ , equivalent to raising the temperature, the system will undergo different states, thus having different lattice structures. In [14], Tao and Jiang have discussed the temperature effect on the monodispersed system, and found it will produce different structures and have different response time. The polydispersed system has rich physics inside.

## VI. DISCUSSION AND CONCLUSION

Here some comments are in order. In experiment, low volume fractions of particles would be realizable as the particles can have a solid hard core and a relatively soft coating by long polymer chains, etc., to avoid self-aggregation. In this sense, the equations and expressions used in this manuscript could be valid, because they were derived in Ref. [24] for low volume fractions and are accordingly valid for chains well separated from each other for estimating the interaction energy between chains tightly packed in different crystalline configurations.

In summary, by using theoretical analysis and molecular dynamics simulations, we investigate the structure of colloidal crystals formed by nonmagnetic particles (or magnetic holes) suspended in a host ferrofluid, by taking into account the effect of polydispersity in size of the particles. We obtain an analytical expression for the interaction energy of monodisperse, bidisperse, and polydisperse inverse ferrofluids. BCT lattices are shown to possess the lowest energy when compared with other sorts of lattices, and thus serve as the ground state of the systems. Also, the effect of particle size distributions (namely, polydispersity in size) plays an important role in the formation of various kinds of structural configurations. Thus, it seems possible to fabricate colloidal crystals by choosing appropriate polydispersity in size. As a matter of fact, it is straightforward to extend the present model to more ordered periodic systems [15], in which the commensurate spacings can be chosen as equal or different.

## Acknowledgments

Two of us (Y.C.J. and J.P.H.) are grateful to Prof. Hua Sun for her valuable discussions. This work was supported by the National Natural Science Foundation of China under Grant No. 10604014. Y.C.J. acknowledges the financial support by Tang Research Funds of Fudan University, and by the "Chun Tsung" Scholar Program of Fudan University. J.P.H. acknowledges the financial support by the Shanghai Education Committee and the Shanghai Education Development Foundation ("Shu Guang" project) under Grant No. KBH1512203, by the Pujiang Talent Project (No. 06PJ14006) of the Shanghai Science and Technology Committee, and by the Scientific Research Foundation for the Returned Overseas Chinese Scholars, State Education Ministry, China.

---

- [1] R. Toussaint, J. Akselvoll, G. Helgesen, A. T. Skjeltorp, and E. G. Flekkøy, *Phys. Rev. E* **69**, 011407 (2004).
- [2] A. T. Skjeltorp, *Phys. Rev. Lett.* **51**, 2306 (1983).
- [3] A. Y. Zubarev and L. Y. Iskakova, *Phys. A* **335**, 314 (2003).
- [4] R. Chantrell and E. Wohlfart, *J. Magn. Magn. Mater.* **40**, 1 (1983).
- [5] Rosensweig, *Annu. Rev. Fluid Mech.* **19**, 437 (1987).
- [6] J. Ugelstad et al, *Blood Purif.* **11**, 349 (1993).
- [7] J. B. Hayter, R. Pynn, S. Charles, A. T. Skjeltorp, J. Trewella, G. Stubbs, and P. Timmins, *Phys. Rev. Lett.* **62**, 1667 (1989).
- [8] A. Koenig, P. Hébraud, C. Gosse, R. Dreyfus, J. Baudry, E. Bertrand, and J. Bibette, *Phys. Rev. Lett.* **95**, 128301 (2005).
- [9] G. Wang and J. P. Huang, *Chem. Phys. Lett.* **421**, 544 (2006).
- [10] G. Wang, W. J. Tian, and J. P. Huang, *J. Phys. Chem. B* **110**, 10738 (2006).
- [11] J. Černák, G. Helgesen and A. T. Skjeltorp , *Phys. Rev. E* **70**, 031504 (2004); G. Helgesen, A. T. Skjeltorp, P. M. Mors, R. Botet, and R. Jullien, *Phys. Rev. Lett.* **61**, 1736 (1988).
- [12] A. P. Hynninen and M. Dijkstra, *Phys. Rev. E* **72**, 051402 (2005).
- [13] R. Tao and J. M. Sun, *Phys. Rev. Lett.* **67**, 398 (1991).
- [14] R. Tao and Q. Jiang, *Phys. Rev. Lett.* **73**, 205 (1994).

- [15] M. Gross and C. Wei, Phys. Rev. E. **61**, 2099 (2000).
- [16] G. L. Gulley and R. Tao, Phys. Rev. E. **56**, 4328 (1997).
- [17] G. L. Gulley and R. Tao, J. of Mod. Phys. B. **15**, 851 (2001).
- [18] W. Wen, N. Wang, H. Ma, Z. Lin, W. Y. Tam, C. T. Chan, and P. Sheng, Phys. Rev. Lett. **82**, 4248 (1999).
- [19] H. J. H. Clercx and G. Bossis, Phys. Rev. E. **48**, 2721 (1993).
- [20] R. Friedberg and Y. K. Yu, Phys. Rev. B. **46**, 6582 (1992).
- [21] H. Sun and K. W. Yu, Phys. Rev. E. **67**, 011506 (2003).
- [22] B. J. de Gans, N. J. Duin, D. van den Ende, and J. Mellema, J. Chem. Phys. **113**, 2032 (2000).
- [23] M. Ota and T. Miyamoto, J. Appl. phys. **76**, 5528 (1994).
- [24] H. Zhang and M. Widom, Phys. Rev. E. **51**, 2099 (1995). Yi-Kuo Yu, Physica A **326**, 522 (2003); T. P. Doerr and Yi-Kuo Yu, Phys. Rev. E **73**, 061902 (2006). The above two referees give detailed method treating surface charge expansion of dielectric spheres.
- [25] O. Mondain-Monval, F. Leal-Calderon, J. Philip, and J. Bibette, Phys. Rev. Lett. **75**, 3364 (1995).
- [26] J. P. Huang and C. Holm, Phys. Rev. E **70**, 061404 (2004).
- [27] T. Kristóf and I. Szalai, Phys. Rev. E. **68**, 041109 (2003).
- [28] *Classical Electrodynamics*, J. D. Jackson, 3rd edition(Wiley, New York, 1999),Chapter 4. For  $m$  is used as magnetic moment, here we use the spherical harmonics  $Y_{ln}$  instead of  $Y_{lm}$ .

## Figure captions

Fig. 1 (color online) Schematic graph showing two nonmagnetic particles (magnetic hole) of radius  $r_1$  and  $r_2$ , suspended in a ferrofluid under an applied magnetic field  $H$ .

Fig. 2 (color online) Three different lattices, bct, fcc, and hcp, which are composed of non-touching particles with different size distribution.

Fig. 3 (color online) The dependence of interaction energy  $U_I(\rho, z)$  (in units of  $\mu_0$ ) versus vertical shift  $z$  for different lattices: (a) bct, (b) fcc, and (c) hcp. In the legend, "dipole-dipole" denotes the case that the dipole-dipole interaction is only considered for calculating the interaction energy.

Fig. 4 (color online) The interaction energy  $U(\rho, z)$  versus lattice constant  $a$ . The solid line stands for the case in which the dipole-dipole interaction is only considered for calculating the interaction energy.

Fig. 5 (color online) The interaction energy per particle  $U(\rho, z)$  versus lattice constant  $a$  for different lattices, bct, fcc, and hcp.

Fig. 6 (color online) (a) The energy gap  $\Delta U = U_{bct} - U_{fcc}$  (in units of  $\mu_0$ ) versus different size of particles in chain A and chain B; (b) The bct lattice energy  $U(\rho, z)$  (in units of  $\mu_0$ ) versus different sizes of particles in chain A and chain B.

Fig. 7 (color online) (a) The ground state interaction energy of a bct lattice versus particle size for random polydispersity configuration (solid line, dashed line, and dotted line) and a configuration composed of two different uniform chains (dashed dotted line and short dashed dotted line). (b) The energy gap  $\Delta U$  between bct and fcc lattices for random polydispersity versus the average particle size  $r_0$ .

Fig. 8. (color online) The configuration of particle distribution at (a) the initial state, (b) the state after 15000 time steps, and (c) the state after 80000 time steps.

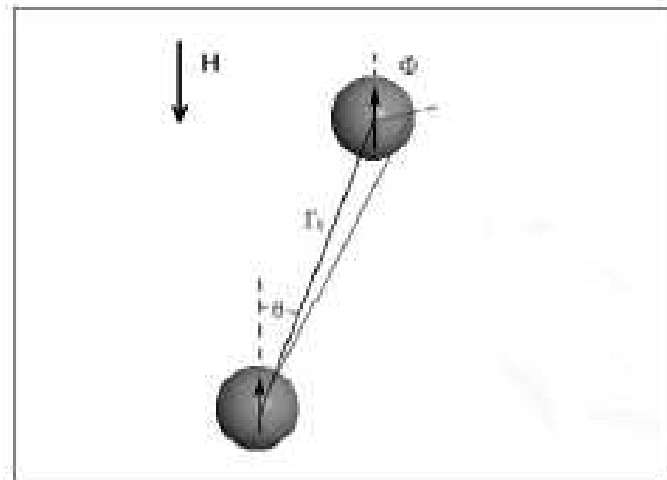


FIG. 1: Jian, Huang, and Tao

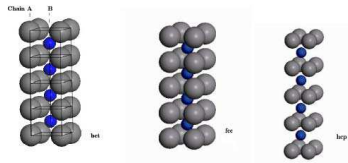


FIG. 2: Jian, Huang, and Tao

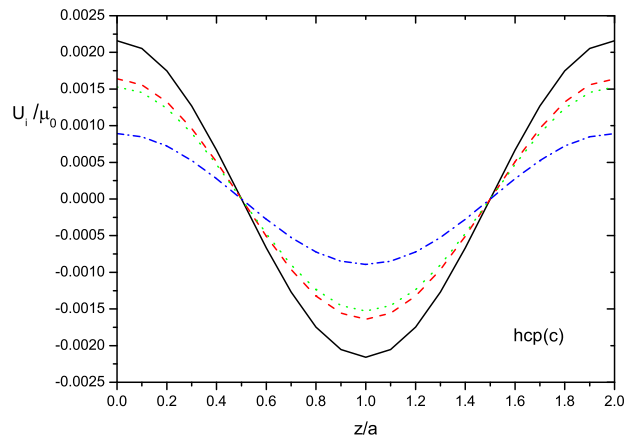
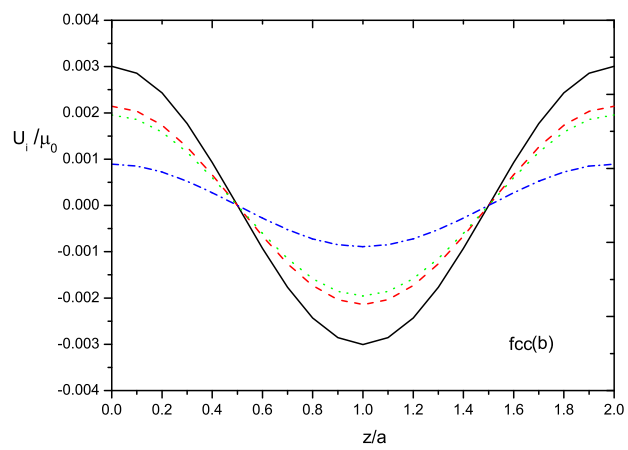
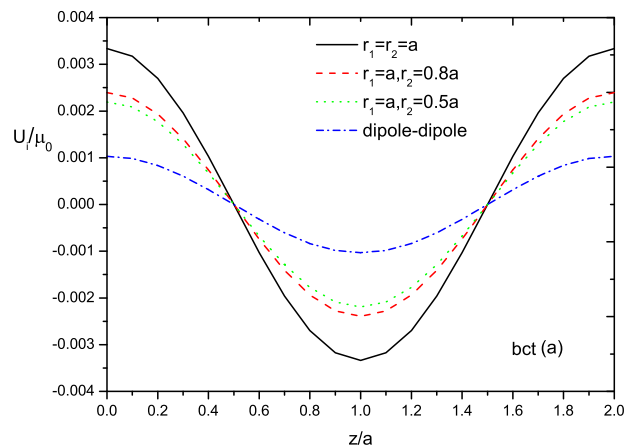


FIG. 3: Jian, Huang, and Tao

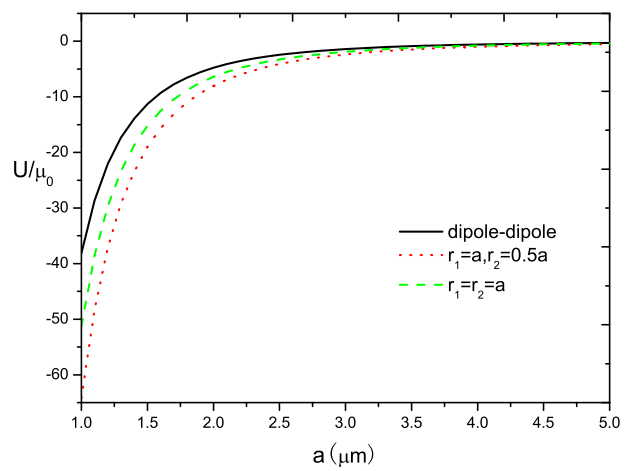


FIG. 4: Jian, Huang, and Tao

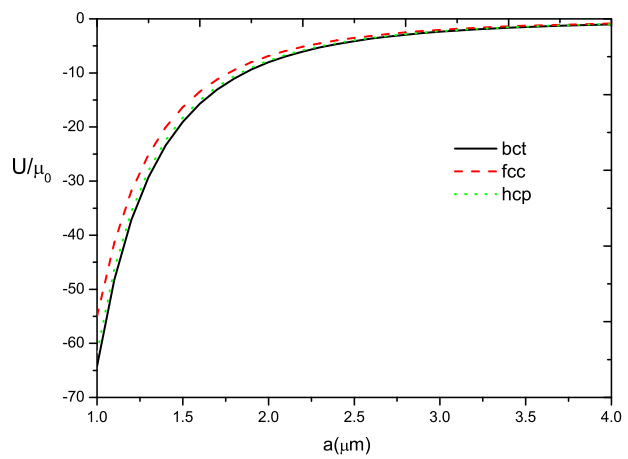


FIG. 5: Jian, Huang, and Tao

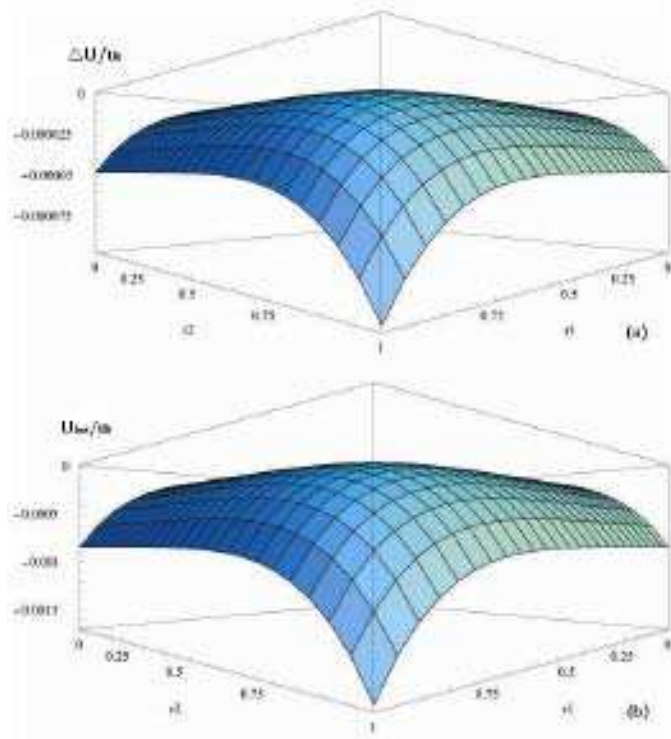


FIG. 6: Jian, Huang, and Tao

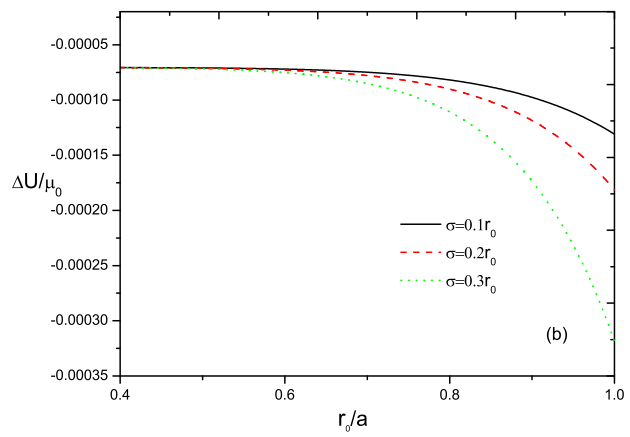
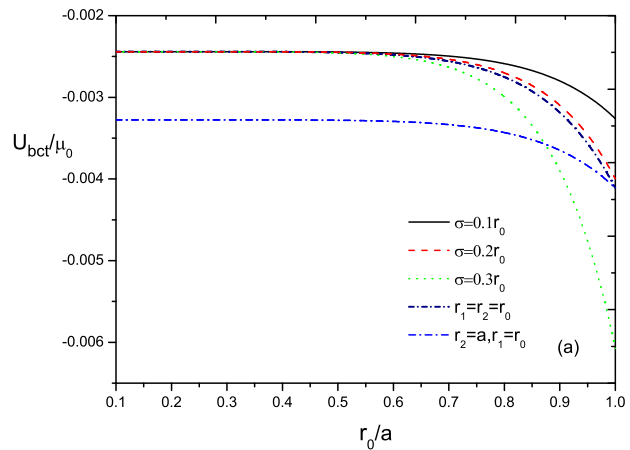


FIG. 7: Jian, Huang, and Tao

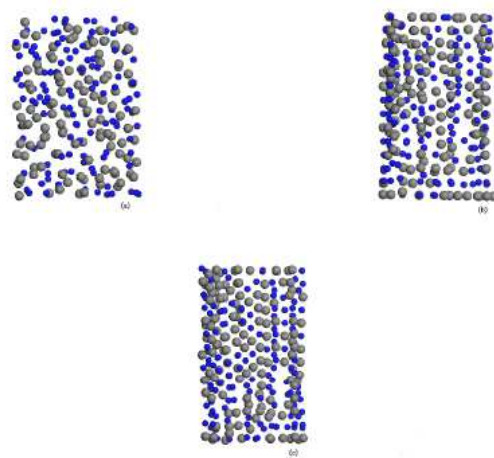


FIG. 8: Jian, Huang, and Tao